Available online at www.sciencedirect.com
ScienceDirect
Trans. Nonferrous Met. Soc. China 30(2020) 2757−2763
Transactions of Nonferrous Metals Society of China
www.tnmsc.cn

Effects of porosity on tensile mechanical properties of porous FeAl intermetallics

Shu-lan SU[1,2], Qiu-hua RAO[1], Yue-hui HE[3], Wei XIE[3]

1. School of Civil Engineering, Central South University, Changsha 410075, China;
2. School of Civil Engineering, Central South University of Forestry and Technology, Changsha 410004, China;
3. State Key Laboratory of Powder Metallurgy, Central South University, Changsha 410083, China

Received 22 November 2019; accepted 28 September 2020

Abstract: Uniaxial tensile tests and scanning electron microscopy (SEM) experiments were carried out on the porous FeAl intermetallics (porosities of 41.1%, 44.2% and 49.3%, pore size of 15−30 μm) prepared by our research group to study the macroscopic mechanical properties and microscopic failure mechanism. The results show that the tensile σ−ε curves of the porous FeAl with different porosities can be divided into four stages: elasticity, yielding, strengthening and failure, without necking phenomenon. The elastic modulus, ultimate strength and elongation decrease with the increase of porosity and the elongation is much lower than 5%. A macroscopic brittle fracture appears, and the microscopic fracture mechanism is mainly intergranular fracture, depending on the Al content in the dense FeAl intermetallics. In addition, the stochastic porous model (SPM) with random pore structure size and distribution is established by designing a self-compiling generation program in FORTRAN language. Combined with the secondary development platform of finite element software ANSYS, the effective elastic moduli of the porous FeAl can be determined by elastic analysis of SPM and they are close to the experimental values, which can verify the validity of the established SPM for analyzing the elastic properties of the porous material.

Key words: porous FeAl intermetallics; uniaxial tensile; fracture mechanism; stochastic porous model (SPM); equivalent elastic modulus

1 Introduction

Fe−Al intermetallics has become a new type of structural material with the wide application prospect [1,2], since it has excellent oxidation resistance, outstanding sulfide resistance [3] and corrosion resistance [4,5] at elevated temperatures [6−8], as well as good processability and weldability [9]. Based on the Kirkendall effect [10,11], the porous FeAl intermetallics has been successfully prepared by partial diffusion/ reactive synthesis sintering process [12,13], which becomes a new type of inorganic porous material following porous ceramics and porous metals [14−16]. In addition, the porous FeAl homogeneous filter membrane with graded-porosity has been made by powder wet spraying technology, and has been widely applied in filtration, separation, purification and extraction under severe environments (such as high temperature, strong corrosion or strong vulcanization) [17−19]. As a new type of functional and structural material, the research on the mechanical properties of the porous FeAl is still in the initial stage [20−22].

Recent research on the mechanical properties of porous material has mainly focused on the model

Foundation item: Project (11502307) supported by the National Natural Science Foundation of China; Project (2016JJ3187) supported by the Natural Science Foundation of Hunan Province, China; Project (50825102) supported by the National Natural Science Funds for Distinguished Young Scholar of China
Corresponding author: Qiu-hua RAO; Tel: +86-13787265488; E-mail: raoqh@mail.csu.edu.cn
DOI: 10.1016/S1003-6326(20)65418-8

analysis method, e.g., geometric structure model [23−26], composite material mechanics model [27] and micropolar theoretical model based on high-order continuum mechanics [28−31], in which the pore structure is considered to be periodically distributed. However, the actual porous material has complicated irregular pore structure. Its macroscopic mechanical properties are related not only to the porosity, but also to the distribution of pore structures. At present, there are only a few literatures available on compressive properties of the porous FeAl. The tensile properties of the porous FeAl are less studied.

In this work, uniaxial tensile tests and scanning electron microscopy (SEM) experiments were carried out to examine the macroscopic tensile properties and microscopic failure mechanism of the porous FeAl with different porosities. The effective elastic modulus of the porous FeAl was calculated by a self-designed generation program of stochastic porous model (SPM) and secondary development platform of finite element software ANSYS for comparison of the experimental results, in order to provide an important theoretical basis for the development and application of the new porous FeAl intermetallics.

2 Experimental

2.1 Preparation of porous FeAl

The raw materials used in this study were 99.8% pure Fe and A1 powders with the particle size of 3−10 μm. These powders were mixed according to the mole ratio of Fe to Al of 6:4 and evenly blended in a cylinder mixer to obtain ultimate composition of FeAl with desired comprehensive properties. The compact discs of *d*32 mm × 3 mm in size were firstly cold pressed by applying 250 MPa and sintered in a vacuum furnace with a vacuum of 2.0×10^{-3} Pa. And then, the compacted powders were heated for 4 h at 1100 °C. Three groups of the porous FeAl with different porosities were prepared. Figure 1 shows the pore morphology of the porous FeAl material by a JSM−6360LV scanning electron microscope (SEM).

2.2 Tensile test

The proportional specimens with the rectangular cross-section of 2 mm × 3 mm and the gauge distance of 14 mm were machined by wire cutting according to the standard of GB/T228—2010 (Fig. 2). For the powder metallurgy material such as the porous FeAl, small-sized specimens were mostly prepared in laboratory tests, because it is difficult to prepare large specimens from the compression moulding to deformation control, and the tensile properties of the material have no relationship with the specimen size. Each specimen was processed by WEDM and polished on SiC sandpaper (mp-300), and the final specimen without visible scratch was obtained for subsequent observation of microstructure and composition, and fully exposed to air for more than 24 h in order to eliminate the influence of wire cutting.

MTS insight biomechanical testing machine was used to conduct tensile test on the porous FeAl tensile specimen (Fig. 3) with maximum load of 1 kN and clamping force of 55.15808 kPa. It can

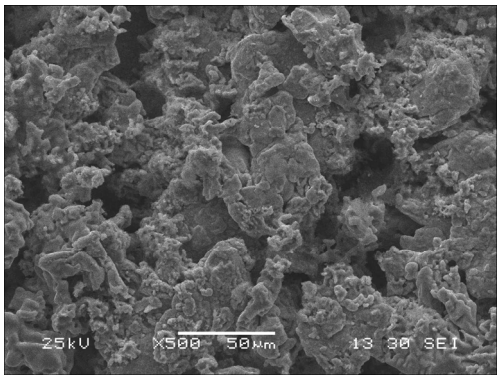

Fig. 1 Micrograph of porous FeAl

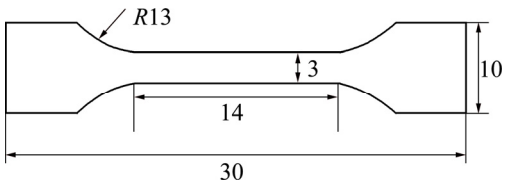

Fig. 2 Size scale of tensile specimen (unit: mm)

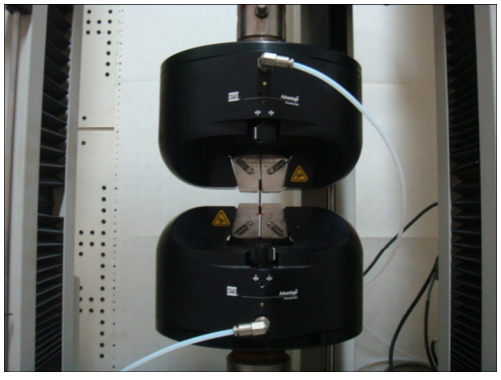

Fig. 3 Tensile test equipment of porous FeAl

measure the strain of small specimen more accurately than the ordinary universal testing machine. The specimens were kept strictly on the central axis of the test machine, and were loaded until failure at rate of 0.5 mm/min. Stress−strain curve was automatically recorded and microscopic characteristics of the fracture surface were analyzed by scanning electron microscope (SEM, JSM−6360LV).

3 Results and discussion

3.1 Analyses of mechanical properties

The porosities (θ) of three groups of the porous FeAl prepared in Section 2.1 were 41.1%, 44.2% and 49.3% separately, measured by the Archimedes method. The pore size distribution was 15−30 μm, measured by mercury intrusion method with Pore Master−60 Quantachrome Instruments.

Uniaxial tensile tests were carried out on the porous FeAl material. Figure 4 shows the stress−strain curves of the porous FeAl with different porosities, where the curves $A_1B_1C_1D_1$, $A_2B_2C_2D_2$, and $A_3B_3C_3D_3$ correspond to the porosities of 41.1%, 44.2%, and 49.3%, respectively. They are all divided into four stages: elasticity (OA), yielding (AB), strengthening (BC) and failure (CD). Compared with the ordinary brittle material, the porous FeAl has some characteristic of low ductility and stable yield stage, closely related to the dense FeAl itself. Its ductility is also influenced by preparation condition, polishing, grinding and machining and other factors. Since the Fe−40at.%Al intermetallics is $B2$-structure of ordered superlattice with the crystal superlattice dislocations, the grain of FeAl is prone to dislocation, deformation or rearrangement to form the directional slip. The balance of the plastic deformation capacity and the strain hardening capacity results in the obvious stable yielding stage.

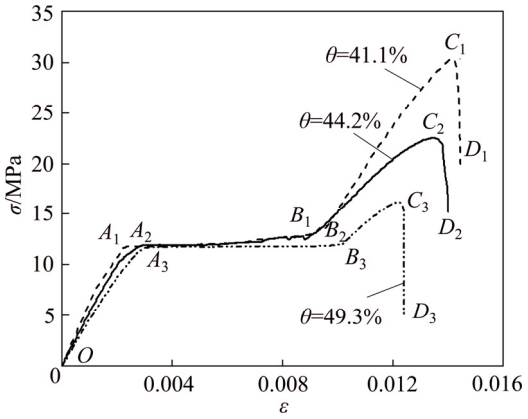

Fig. 4 Stress−strain curves of porous FeAl with different porosities

Table 1 lists the main mechanical properties of the porous FeAl material. It is seen that the elastic modulus (E_{ev}), ultimate strength (σ_b) and elongation (δ) are decreased with the increase of porosity (θ). Obviously, the larger the porosity (θ), i.e., the less the solid material in unit volume, the weaker the ability to resist deformation of the porous material and thus the lower the mechanical properties. The yield strength (σ_s) is changed very little with the porosity (θ), since the yielding of the porous FeAl depends largely on the slipping deformation of the dense body.

Table 1 Tensile mechanical properties of porous FeAl with different porosities

No.	θ/%	E_{ev}/GPa	σ_s/MPa	σ_b/MPa	δ/%
1	41.1	6.3	11.8	30.7	1.44
2	44.2	5.4	11.9	22.5	1.38
3	49.3	4.7	11.7	16.3	1.24

3.2 Fractographic analysis

Figure 5 shows the fractured specimen of the porous FeAl, where the flat fractured surface is approximately perpendicular to the tensile direction and the failure process has no necking. The elongation rate is much smaller than 5%, showing typical brittle fracture in macroscopy.

Fig. 5 Tensile fracture specimen of porous FeAl

Figure 6 shows the SEM fracture morphologies of the porous FeAl with different porosities. All of them have the same intergranular fracture with a large number of crystal sugar-like morphology, which is closely related to the Al content in the dense FeAl material [1]. When the content of Al is 36.5 at.%, the fracture of the dense FeAl material in air is transgranular fracture. When the content of Al increases from 36.5 to 40 at.%, the

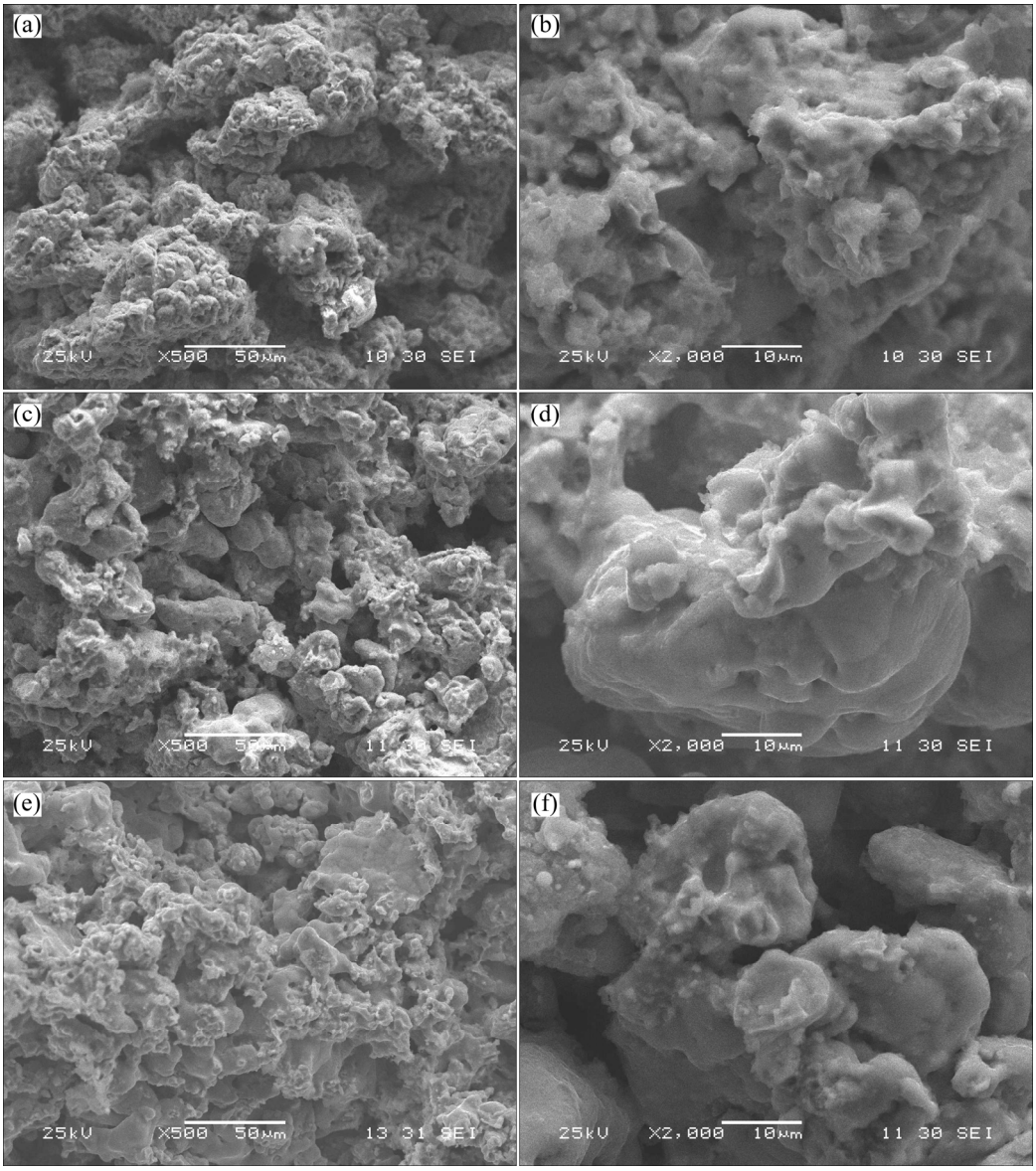

Fig. 6 SEM fracture morphologies of porous FeAl with different porosities in tension: (a, b) θ=41.1%; (c, d) θ=44.2%; (e, f) θ =49.3%

strength of grain boundary is gradually weakened, and the fracture changes from transgranular to intergranular fracture. Therefore, the microscopic characteristic of tensile fracture of Fe−40at.%Al porous material in air in this experiment is mainly intergranular fracture.

4 Finite element analyses

4.1 Stochastic porous model

The porosities of the porous model are the same as those of the porous FeAl prepared in the Section 2.1 (θ=41.1%, 44.2%, 49.3%, respectively). In order to facilitate modeling, the pore structure of the model is assumed to be circular, and the model and pore sizes are enlarged by 100 times at the same time, which does not affect the results. The size of the porous model is 100 mm × 50 mm × 1 mm, and the radius of the circular pore (r) varies from 1 to 3 mm. When the porosity and the radius range are given, the parameters of circular pore in the model (the number of circular pores, the radius of circular pores and the coordinates of circle center) are firstly obtained by using FORTRAN language, and then the random pore model with random pore size and distribution is generated by using finite element software ANSYS, as shown in Fig. 7.

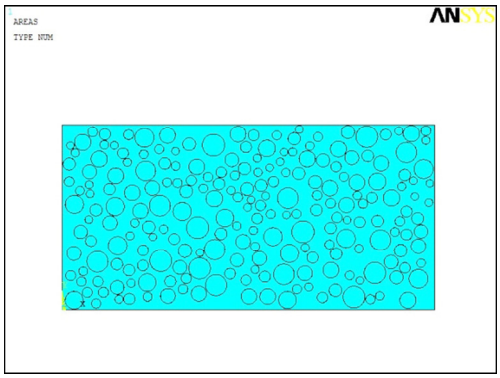

Fig. 7 Stochastic porous model

4.2 Calculation of elastic modulus

The elastic modulus of the porous FeAl can be obtained by using finite element software ANSYS to simulate the uniaxial tensile test of the stochastic porous model.

The SPM is considered as composition of the dense FeAl and circular pore, where the elastic constitutive relationship is adopted for the dense FeAl. Its mechanical properties can be obtained by the tested tensile stress−strain curve: elastic modulus E_s=39 GPa and Poisson ratio μ_s=0.234. Considering that the boundary of a circular hole is a curve, six- or eight-nodes plane quadrilateral element PLANE183 was selected for finite element mesh generation. When the free mesh generation is adopted, the mesh size needs to be adjusted to reduce the number of elements and nodes in order to reduce the amount of calculation without affecting the accuracy. The boundary condition of the model is that: the left side has fixed horizontal displacement and the lower side has fixed vertical displacement. The nodes on the right side are coupled and loaded by a uniform tensile force of 20 N in horizontal direction, as shown in Fig. 8.

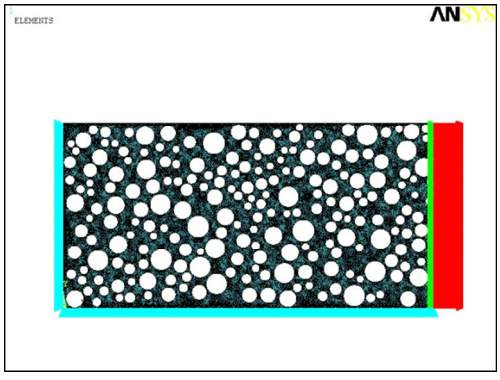

Fig. 8 Loading figure of SPM

Based on the elastic analysis of SPM, the horizontal displacement is obtained (Fig. 9), and the resultant force (F) and the displacement (u) in loading direction on the right side of the model are also extracted from the calculation results. Therefore, the effective elastic modulus (E_{cv}) of the porous FeAl can be calculated by the following formula, as listed in Table 2.

$$E_{cv}=\frac{\sigma}{\varepsilon}=\frac{F/A_0}{u/l_0} \quad (1)$$

where A_0 and l_0 are the original area and length of the mode, respectively.

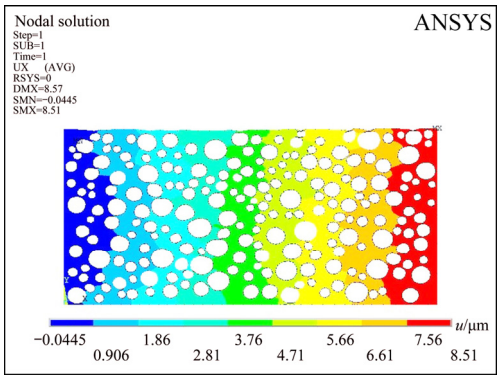

Fig. 9 Displacement deformation map of SPM

Table 2 Effective elastic modulus of porous FeAl

No.	θ/%	F/N	u/μm	E_{cv}/GPa
1	41.1	39640	8.2344	9.6
2	44.2	40560	9.1013	8.9
3	49.3	39760	11.552	6.8

Comparison of Table 1 and Table 2 indicates that the calculated effective elastic moduli (E_{cv}) of the porous FeAl with different porosities are close to the experimental values (E_{ev}), which can verify the validity of the established stochastic porous model (SPM) for analyzing the elastic properties of the porous material. Since the SPM does not take into account the influence of irregular shape and defects of the actual pores, E_{cv} is higher than E_{ev}.

5 Conclusions

(1) The tensile stress−strain curves of the porous FeAl with different porosities have the same four stages: elasticity, yielding, strengthening and failure. The elastic modulus, ultimate strength and elongation are decreased with the increase of porosity. The yield strength changes very little

when the difference of porosity is small.

(2) The tensile fracture surface of the porous FeAl is relatively flat without necking phenomenon before failure, and the elongation is much lower than 5%, which is a macroscopic brittle fracture. The microscopic fracture mechanism is mainly intergranular fracture, depending on the Al content in the dense FeAl.

(3) The stochastic porous model (SPM) with random pore structure size and distribution is established by designing a self-compiling generation program in FORTRAN language. Combined with the secondary development platform of finite element software ANSYS, the effective elastic modulus of the porous FeAl can be determined by elastic analysis of SPM. The calculated equivalent elastic moduli of the porous FeAl with different porosities are close to the experimental values, which can verify the validity of the established SPM for analyzing the elastic properties of the porous material.

References

[1] LIU Wen-juan, WANG Yu, GE Hong-bin, LI Li, DING Yi, MENG Ling-gang, ZHANG Xing-guo. Microstructure evolution and corrosion behavior of Fe−Al-based intermetallic aluminide coatings under acidic condition [J]. Transactions of Nonferrous Metals Society of China, 2018, 28: 2028−2043.

[2] PENG Chao-qun, HUANG Bai-yun, HE Yue-hui. Progress in studies on Ni−Al, Fe−Al and Ti_3Al intermetallics [J]. Special Casting and Nonferrous Alloys, 2001, 6: 27−29. (in Chinese)

[3] LANG F Q, YU Z M, GEDEVANISHVILI S, DEEVI S C, HAYASHI S, NARITA T. Sulfidation behavior of Fe−40Al sheet in H_2−H_2S mixtures at high temperatures [J]. Intermetallics, 2004, 12: 469−475.

[4] AMAYA M, ESPINOSA-MEDINA M A, PORCAYO-CALDERON J, MARTINEZ L, GONZALEZ-RODRIGUEZ J G. High temperature corrosion performance of FeAl intermetallic alloys in molten salts [J]. Materials Science and Engineering A, 2003, 349: 12−19.

[5] ZHU Xiao-lin, YAO Zheng jun, GU Xue-dong, CONG Wei, ZHANG Ping-ze. Microstructure and corrosion resistance of Fe−Al intermetallic coating on 45 steel synthesized by double glow plasma surface alloying technology [J]. Transactions of Nonferrous Metals Society of China, 2009, 19: 143−148.

[6] ZHANG Yong-gang, HAN Ya-fang, CHEN Guo-liang, GUO Jian-ting, WAN Xiao-jing, FENG Di. Structural intermetallics [M]. Changsha: National Defence Industry Press, 2001. (in Chinese)

[7] XU C H, GAO W, HE Y D. High temperature oxidation behavior of FeAl intermetallics-oxide scales formed in ambient atmosphere [J]. Scripta Materialia, 2000, 42: 975−980.

[8] LANG F Q, YU Z M, GEDEVANISHVILI S, DEEVI S C, NARITA T. Isothermal oxidation behavior of a sheet alloy of Fe−40at.%Al at temperatures between 1073 and 1473 K [J]. Intermetallics, 2003, 11: 697−705.

[9] AMILS X, NOGUEÂS J, SURINÄCH S, BAROÁ M D, MUNÄOZ-MORRIS M A, MORRIS D G. Hardening and softening of FeAl during milling and annealing [J]. Intermetallics, 2000, 8: 805−813.

[10] PAUL A, van DAL M J H, KODENTSOV A A, van LOO F J J. The Kirkendall effect in multiphase diffusion [J]. Acta Materialia, 2004, 52: 623−630.

[11] BOUAYAD A, GEROMETTA Ch, BELKEBIR A, AMBARI A. Kinetic interactions between solid iron and molten aluminium [J]. Materials Science and Engineering A, 2003, 363: 53−61.

[12] GAO Hai-yan. Investigations on Fe−Al intermetallic compound porous material [D]. Changsha: Central South University, 2009: 37−47. (in Chinese)

[13] GAO Hai-yan, HE Yue-hui, ZOU Jin, XU Nan-ping, LIU C T. Tortuosity factor for porous FeAl intermetallics fabricated by reactive synthesis [J]. Transactions of Nonferrous Metals Society of China, 2012, 22: 2179−2183.

[14] LIU Ya-nan, SUN Zhi, CAI Xiao-ping, JIAO Xin-yang, FENG Pei-zhong. Fabrication of porous FeAl-based intermetallics via thermal explosion [J]. Transactions of Nonferrous Metals Society of China, 2018, 28: 1141−1148.

[15] SHEN P Z, SONG M, GAO H Y, HE Y H, ZOU J, XU N P, JIANG Y, HUANG B Y, LIU C T. Structural characteristics and high-temperature oxidation behavior of porous Fe−40at.%Al alloy [J]. Journal of Material Science, 2009, 44: 4413−4421.

[16] SHEN Pei-zhi, GAO Ling, GAO Hai-yan, HE Yue-hui. High-temperature sulfidation behavior and application in SO_2-containing gas cleanup of porous FeAl intermetallics [J]. Materials Science and Engineering of Powder Metallurgy, 2010, 15: 38−43. (in Chinese)

[17] GAO Hai-yan, HE Yue-hui, SHEN Pei-zhi, JIANG Yao, HUANG Bai-yun, XU Nan-ping. Welding of FeAl porous material and stainless steel [J]. The Chinese Journal of Nonferrous Metals, 2009, 19: 90−95. (in Chinese)

[18] HE Yue-hui, JIANG Yao, GAO Hai-yan, SHEN Pei-zhi, XU Nan-ping, HUANG Bai-yun. A preparation method of pore gradient homogeneous FeAl filter membrane [P]. Chinese patent, 200710035404.4. 2008−1−23. (in Chinese)

[19] SHEN P Z，HE Y H, GAO H Y, ZOU J, XU N P，JIANG Y，HUANG B Y，LIU C T. Development of a new graded-porosity FeAl alloy by elemental reactive synthesis [J]. Desalination 2009, 249: 29−33.

[20] SU Shu-lan, RAO Qiu-hua, HE Yue-hui. Theoretical prediction of effective elastic constants for new intermetallic compound porous material [J]. Transactions of Nonferrous Metals Society of China, 2013, 23: 1090−1097.

[21] SU Shu-lan, RAO Qiu-hua, HE Yue-hui, ZHANG Hui-bin. Elastic modulus for new FeAl porous material based on micropolar theory [J]. Journal of Central South University (Science and Technology), 2018, 49: 301−306. (in Chinese)

[22] SU Shu-lan, RAO Qiu-hua, HE Yue-hui. Compression mechanical properties of FeAl intermetallic compound porous material [J]. Rare Metal Materials and Engineering, 2018, 47: 2453−2457. (in Chinese)
[23] CHUANG C H, HUANG H S. Elastic moduli and plastic collapse strength of hexagonal honeycombs with plateau borders [J]. International Journal of Mechanical Sciences, 2002, 44: 1827−1844.
[24] LIU Pei-sheng, CUI Guang, CHEN Wei. Study on property model for porous materials 1: Mathematical relations [J]. Journal of Materials Engineering, 2019, 47(6): 42−62. (in Chinese)
[25] LIU Pei-sheng, XIA Feng-jin, CHEN Wei. Study on property model for porous materials 2: Experimental verification [J]. Journal of Materials Engineering，2019, 47(7): 35−49. (in Chinese)
[26] LIU Pei-sheng, YANG Chun-yan, CHEN Wei. Study on property model for porous materials 3: Mathematical deduction [J]. Journal of Materials Engineering, 2019, 47: 59−81. (in Chinese)
[27] LU Zi-xing, HUANG Zhu-ping, WANG Ren. The theoretical prediction of compressive young's moduli for polyurethane foam plastics[J]. Chinese Journal of Applied Mechanics, 1996, 13: 8−13. (in Chinese)
[28] RAMAKRISHNAN N, ARUNACHALAM V S. Effective elastic moduli of porous solid [J]. Journal Materials Science, 1990, 25: 3930−3937.
[29] WANG X L, STRONGE W J. Micropolar theory for two-dimensional stresses in elastic honeycomb [J]. The Royal Society, 1999, 455: 2091−2116.
[30] OSTOJIA-STARZEWSKI M. Lattice models in micromechanics [J]. Applied Mechanics Review, 2002, 55: 35−60.
[31] KUMAR R S, MCDOWELL D L. Generalized continuum modeling of 2-D periodic cellular solids [J]. International Journal of Solids and Structures, 2004, 41: 7399−7422.

孔隙率对 FeAl 金属间化合物多孔材料拉伸力学性能的影响

苏淑兰[1,2]，饶秋华[1]，贺跃辉[3]，谢 维[3]

1. 中南大学 土木工程学院，长沙 410075；
2. 中南林业科技大学 土木工程学院，长沙 410004；
3. 中南大学 粉末冶金国家重点实验室，长沙 410083

摘 要：针对本课题组制备的 FeAl 金属间化合物多孔材料(孔隙率为 41.1%、44.2% 和 49.3%，孔径为 15~30 μm)开展单轴拉伸实验和扫描电镜实验，研究其宏观力学性能和微观破坏机理。结果表明：不同孔隙率下 FeAl 多孔材料拉伸 σ–ε 曲线均可分为弹性、屈服、强化和破坏 4 个阶段，没有颈缩现象，其弹性模量、强度极限和伸长率均随孔隙率的增大而减小；其伸长率远低于 5%，为宏观脆性断裂。微观上以沿晶断裂为主，其微观断裂机理取决于 FeAl 金属间化合物致密材料中的 Al 含量。此外，利用 FORTRAN 语言自编计算程序生成孔隙大小和分布具有随机性的随机孔隙模型。结合 ANSYS 有限元软件二次开发平台，对随机孔隙模型进行弹性分析，得到 FeAl 多孔材料的等效弹性模量，计算所得的弹性模量值与实验值较为接近，说明建立的随机孔隙模型分析多孔材料的弹性性能是可靠的。

关键词：FeAl 多孔金属间化合物；单轴拉伸；断裂机理；随机孔隙模型；等效弹性模量

(Edited by Xiang-qun LI)